

Observations of giant outbursts from Cygnus X-1

S. Golenetskii, R. Aptekar, D. Frederiks, E. Mazets, and V. Palshin

Ioffe Physico-Technical Institute, St. Petersburg, 194021, Russia

`golen@pop.ioffe.rssi.ru`

K. Hurley

University of California, Berkeley, Space Sciences Laboratory, Berkeley, CA 94720-7450

T. Cline

NASA Goddard Space Flight Center, Code 661, Greenbelt, MD 20771

B. Stern¹

Institute for Nuclear Research, Moscow 117312, Russia

Received _____; accepted _____

¹Stockholm Observatory, SE-133 36, Saltsjöbaden, Sweden

ABSTRACT

We present interplanetary network localization, spectral, and time history information for 6 episodes of exceptionally intense gamma-ray emission from Cygnus X-1. The outbursts occurred between 1995 and 2002, with durations up to ~ 28000 seconds. The observed 15 - 300 keV peak fluxes and fluences reached 3×10^{-7} erg cm $^{-2}$ s $^{-1}$ and 8×10^{-4} erg cm $^{-2}$ respectively. By combining the triangulations of these outbursts we derive an ~ 1700 square arcminute (3σ) error ellipse which contains Cygnus X-1 and no other known high energy sources. The outbursts reported here occurred both when Cyg X-1 was in the hard state as well as in the soft one. The spectral data indicate that these giant flares display the same parameters as those of the underlying hard and soft states, suggesting that the flares represent another manifestation of these states.

Subject headings: black hole physics - stars: individual (Cygnus X-1)

1. Introduction

Cygnus X-1 is known to exhibit two states of X-ray emission. The first, more common one, is the hard state, in which the 20 - 200 keV flux is roughly one Crab, and the <10 keV emission is about 0.5 Crab. The second is the soft state, in which the low energy X-ray flux increases by a factor of 2 - 4, while the high energy flux decreases by a factor of about 2. Transitions between the two states and flaring have been documented extensively (Ling et al. 1997; Zhang et al. 1997; Cui et al. 2002; McConnell et al. 2002), and both states exhibit variability of a factor of two or so on all timescales. The source is a high mass X-ray binary and a black hole candidate (Liang and Nolan 1984), and the high energy emission is powered by accretion. Its distance from Earth is approximately 2 kpc.

In this paper we report on six episodes of long, intense gamma-ray emission from this source; we refer to them as *outbursts* to distinguish them from the shorter, less intense flaring which has been documented previously. One of these outbursts, 950325, was found by Mazets et al. (2001) and initially thought to be a gamma-ray burst; subsequently, however, its source was found to be Cygnus X-1 by M. Briggs (private communication, 1995). Later, Stern et al. (2001) called attention to five outbursts on 1999 April 19-21. During the two brightest events, the hard X-ray flux increased by over an order of magnitude for ~ 1000 s. Observations by *Ulysses* and *Konus - Wind* of still two more outbursts in 2002 have prompted us to reanalyze all the available data in order to obtain better energy spectra and a more precise source location as well.

2. Observations

The outbursts reported here were discovered in the time history data of the gamma-ray burst (GRB) detectors aboard the *Wind*, *Ulysses*, and *Compton Gamma-Ray Observatory* (CGRO) spacecraft (*Konus*, GRB, and the Burst and Transient Source Experiment, or BATSE, experiments respectively). In general, the data used were for the non-triggered modes, with low temporal and spectral resolution (0.25 - 2.9 s and 3 channels, respectively). Although in some cases, the emission was intense enough to trigger BATSE, the data obtained in the triggered modes had too small a duration to cover the entire outburst, and the lower time resolution continuous data have been used for most of our analysis. Table 1 gives the dates, times, and durations of the six events, as well as the spacecraft which observed them. To determine the source of the outbursts, we have employed the usual method of interplanetary network (IPN) triangulation for a repeating source (e.g. Hurley et al. 1999). In all cases, the IPN consisted of only two widely separated spacecraft, so a single annulus of location was obtained for each flare. The six annuli were combined

statistically to produce the 1, 2, and 3 σ error ellipses shown in figure 1. The only known hard X-ray source in this region is Cyg X-1, which lies at the $\sim 95\%$ confidence level.

Since the Konus detector observed 5 of the 6 outbursts in table 1 (one outburst, 990421B, occurred during a period where the data were contaminated by solar particles), we have used the data from it exclusively for time-resolved spectral analysis. For four cases we have used the 3 channel data (nominally 10-50, 50-200, and 200-750 keV, or G1, G2, and G3, respectively) which span the entire event. In the fifth case (950325) a cosmic gamma-ray burst (GRB) fortuitously triggered Konus during the flare, allowing it to record multi-channel energy spectra for a total of 360 s, starting 120 s after the GRB trigger, when the 15 s long GRB had ceased emitting. In addition, for this event, there are also 3 channel data. Because the most detailed data are available for it, we discuss this outburst first.

The 950325 outburst is presented in detail in figure 2. In the top three panels, the time histories in the G1, G2, and G3 windows are shown, and in the bottom panels, the hardness ratios G2/G1 and G3/G2. The letters A-D indicate the intervals where energy spectra have been analyzed. (The results of this and other analyses are summarized in table 2.) In particular, B marks the 360 s interval where multi-channel spectra were accumulated. The gap following B is the interval where the data were transferred to the onboard tape recorder. The hardness ratios display a weak but obvious spectral variability. From them, it is reasonable to assume that the multi-channel energy spectra measured in interval B, during the fading stage of the flare, also characterize the spectrum of the preceding, intense phase. The multi-channel spectrum is presented in figure 3 in νF_ν units. (The spectral deconvolution procedure has been described by Terekhov et al. 1998). The solid line gives the best fit spectrum, $E^2 A (E/1\text{keV})^{-\alpha} \exp(-E/E_0) \text{ keV cm}^{-2} \text{ s}^{-1}$, with $A = 0.88 \pm 0.40 \text{ photons cm}^{-2} \text{ s}^{-1} \text{ keV}^{-1}$, $\alpha = 1.24 \pm 0.15$, and $E_0 = 112 \pm 30 \text{ keV}$, and with $\chi^2 = 22.6$ for 18 degrees of freedom. This

spectral shape is consistent with that of the Cyg X-1 hard state.

The 15 - 300 keV time histories of the other outbursts are presented in figures 4 - 8. The vertical dotted lines and letters at the top of the Konus plots indicate the intervals over which 3 channel energy spectra were accumulated to improve statistics. Fits were done with the function $A(E/1\text{keV})^{-\alpha}\exp(-E/E_0)$ photons $\text{cm}^{-2} \text{s}^{-1}$, and the fitting parameters are given in table 2. E_p , the peak energy, was obtained from the spectrum expressed in νF_ν units. The fluences and peak fluxes, given in table 3, were calculated assuming no spectral evolution over the intervals considered.

It should be noted that an omnidirectional sensor detects an outburst from a source as a temporary increase in the count rate over an average background level. Clearly in this case that level includes any persistent flux from Cyg X-1. Thus the total flux during an outburst will be the sum of the persistent and flaring fluxes detected by Konus. However, the value of the persistent flux from Cyg X-1 at time intervals adjacent to the outburst is poorly known. Accordingly the fluences and peak fluxes in table 3 are only to be considered estimates of the outburst component.

3. Discussion

Long-term observations of Cyg X-1 in X-rays and soft gamma-rays from HEAO 3 (Ling et al. 1987), BATSE (Ling et al. 1997), Mir-Kvant (Borkus et al. 1995), and BeppoSAX (Frontera et al. 2001) have shown that the source spends most of the time in the hard state. According to BATSE data for 1991 - 1999 (McConnell et al. 2002), the hard flux in the 20 - 100 keV energy range varied between 0.2 and 0.36 photons $\text{cm}^{-2} \text{s}^{-1}$, roughly the average value corresponding to the γ_2 level in the 45 - 140 keV band identified by Ling et al. (1987). In 1999 April, several outbursts lasting up to 1000 s were found in the BATSE data (Stern

et al. 2001). The peak fluxes in the 50 - 300 keV range, $0.3 - 1.1 \text{ photons cm}^{-2} \text{ s}^{-1}$, were significantly higher than the average value of $\sim 0.1 \text{ photons cm}^{-2} \text{ s}^{-1}$. Transitions to the soft state lasting for several months were observed only a few times. According to the data of the All Sky Monitor aboard the *Rossi X-ray Timing Explorer* (RXTE/ASM) (McConnell et al. 2002), the soft X-ray (2 - 10 keV) count rates increase from ~ 20 to $\sim 80 \text{ counts s}^{-1}$ after transitions to the soft state. From the BATSE and RXTE light curves we have ascertained that outbursts 950110, 950325, and 990421A and B occurred while Cyg X-1 was in the hard state whereas outbursts 020224 and 020331 arose from the soft state.

Broadband spectral observations of Cyg X-1 from numerous spacecraft and combinations of spacecraft have been used to study comprehensively the spectral shapes at various times in order to deduce the emission mechanism and the geometry of the regions emitting and reprocessing radiation (Mir-Kvant: Borkus et al. 1995; CGRO: Ling et al. 1997; Ginga and CGRO: Gierlinski et al. 1997; RXTE: Dove et al. 1998; ASCA, RXTE, and CGRO: Gierlinski et al. 1999; BeppoSAX: Frontera et al. 2001; and CGRO and BeppoSAX: McConnell et al. 2002). The accuracy of our data is insufficient for such a thorough analysis of source models. Rather, we have focused on obtaining the essential information on a new feature of Cyg X-1 activity from limited observational data using the simplest model spectra, namely a power law, $AE^{-\alpha}$, or a power law with an exponential cutoff, $AE^{-\alpha}\exp(-E/E_0)$. Apart from the lack of high resolution spectral data, the most serious difficulties in our data processing are connected with slow changes in the background level, especially in the low energy ranges. Background count rates in the G1 window and, to a lesser extent, in G2, are strongly affected by the activity of cosmic X-ray sources and vary, even when the Sun is quiet, by $\pm 1\%$, averaged over hours and days. For this reason, for example, we do not attempt spectral fits for the long, weak onsets of outbursts 950110 and 950325.

The intense stage of each outburst was subdivided into several time intervals in some concordance with the temporal behaviour of the hardness ratio, as shown in figures 3-8. Spectral parameters for all of these intervals were determined by fitting the numbers of counts accumulated in energy bands G1, G2, and G3 using the response function of the detector. To estimate the uncertainties in the parameters, the covariance matrix was computed. In the case of the exponentially attenuated power law, parameters α and E_0 are strongly correlated. The peak energy E_p for a νF_ν spectrum is a more robust characteristic. Estimates of the uncertainties were checked and confirmed by numerical simulations.

All of these data are collected in table 2, which includes an additional interval B* for 950325. This interval, where G1, G2, and G3 data were available, partially overlaps interval B. From this it is evident that the parameters obtained by both methods agree well to within their uncertainties. The 15 - 300 keV fluences and peak fluxes for all the outbursts are presented in table 3.

The main conclusions which can be drawn from these data are the following.

- An exponential cutoff is essential when fitting outbursts arising from the hard state. The parameters α and E_0 are consistent with the values for the hard state of Cyg X-1 reported in literature.
- The energy spectra of the 2002 outbursts, when Cyg X-1 had gone into the soft state, are much softer in our energy range. The spectra of 020331 are well fit by a single slope power law with $\alpha \sim 2.6$. The spectra of 020224 display a low E_0 with large uncertainties in α . This probably reflects a flattening of the νF_ν spectrum in the ~ 10 - 30 keV range often observed in the soft state (Gierlinski et al. 1999).
- In general, it seems that giant outbursts from Cyg X-1 maintain the spectral parameters, and hence emission mechanism, of their current underlying spectral

state, even though the 15 - 300 keV peak fluxes are up to ten times higher than the persistent emission fluxes. The corresponding fraction of the peak luminosity in these outbursts approaches one tenth of the Eddington luminosity for an object with $M/M_{\odot} \sim 10$.

The soft and hard states of Cygnus X-1 and other galactic black hole candidates have comparable bolometric luminosities, but different energy spectra (e.g. Ling et al. 1997; Zdziarski et al. 2002). The hard X-ray spectra of these sources are typically characterized by fitting parameters $\alpha = 1.6$, $E_p = 150$ keV (Gierlinski et al. 1999), which are consistent with those in table 2 for the first four outbursts. Many authors have interpreted them as thermal Comptonization with optical depth $\tau_T \sim 1$ and electron temperature $\sim 50 - 100$ keV (for recent studies see Maccarone & Coppi, 2002).

The model for transitions between the soft and hard states discussed in a number of recent works is based on the idea of accretion disk transformations. In the soft state the accretion proceeds via a standard optically thick accretion disk (Shakura & Sunyaev, 1973) emitting a blackbody soft X-ray peak and a nonthermal tail resulting from coronal activity in the disk. In the hard state the inner part of the disk is thought to form a hot geometrically thick corona (see e.g. Barrio, Done & Nayakshin, 2000, Poutanen, Krolik & Ryde, 1997, and references therein) with a moderate ($\tau_T \sim 1$) optical depth. The outer region of the disk, beyond a few tens to one hundred gravitational radii, still remains optically thick emitting a cooler (0.1 - 0.2 keV) and weaker blackbody component. The physical grounds for such a transformation could be a transition of the inner part of the disk into a regime balancing between ADAF and standard disk modes (Esin et al. 1998). However such a regime requires a fine tuning which would clearly be violated during giant outbursts (Stern, Beloborodov & Poutanen, 2001).

An alternative to disk accretion for the case of the hard state can be accretion of the

companion wind with a near-critical angular momentum (Illarionov & Sunyaev, 1975). Then, instead of a standard optically thick disk, a small-scale disk with $\tau_T \sim 1$ can appear. This scenario can naturally describe the hard state spectrum (Beloborodov & Illarionov, 2001). No difficulties with the large observed variabilities arise in this model.

What triggers the giant outbursts? The most straightforward suggestion is that this could be some rare eruptive phenomenon in the donor wind ejection. The typical dynamical timescale for standard disk accretion in the case of Cyg X-1 is much longer than the duration of the outbursts, such that any fluctuations in donor ejection rate would be dilated by up to a day or more (Bisnovaty-Kogan, private communication, 2002). The direct wind accretion, on the contrary, has dynamical timescale ~ 1000 s but a shorter timescale can arise from instabilities of the accreting flow (Illarionov, private communication, 2002).

The cases of outbursts 020224 and 020231, detected during the soft state, are more challenging. Most of the outbursts have similar properties, which hints at a common nature. In this case, however, the evidence for a full scale optically thick disk is very strong. This leads us to suggest that direct wind accretion can co-exist with the standard disk. If this is correct, the soft X-ray thermal emission should not change substantially during outbursts in the soft state. To summarize we can state that the observation of outbursts supports the wind accretion model over standard disk accretion, but the detection of hard outbursts during the soft state complicates the interpretation.

Other interpretations are possible. For example, the outbursts can be attributed to the recently discovered jet of Cyg X-1 (Stirling et al. 2001) and their recurrence could be explained by its precession (Romero, Kaufman Bernardo & Mirabel, 2002).

4. Conclusion

The outbursts reported here have durations comparable to the period of a low Earth-orbiting spacecraft, making them difficult to detect and follow from experiments aboard such spacecraft, but relatively easy for experiments which are far from Earth and do not undergo occultation and orbital background variations. Indeed, our observations of 990421A show that it continues well beyond the point at which it was Earth-occulted to BATSE, and our observations of 990421B indicate that it commenced several hundred seconds before it rose on BATSE (Stern et al. 2001). These observations point to a new use for the IPN, namely tracking long, intense flares from Galactic transients. The data from a single experiment which has little or no directional and/or spectral information are easily confused with solar X-ray and particle events, which explains why it has taken so long to determine the origin of some of the outbursts presented here. However, confirmation by a second spacecraft solves this problem and gives an annulus of position which in many cases may be sufficient to determine the origin of the emission. For several outbursts, the BATSE observations alone yield source directions which are only accurate to 17° , leaving the possibility that the source could have been Cygnus X-3. However, relatively small error ellipses may be obtained from multiple observations, and our localizations rule this out conclusively.

The histories of Cygnus X-1 and GRBs have been curiously intertwined over the decades. In the early days of X-ray astronomy, the use of interplanetary spacecraft was suggested to localize sources with rapid time variations such as Cyg X-1 (Giacconi 1972). Although, to our knowledge, such measurements were never carried out on persistent X-ray sources, today the technique is the basis of the IPN, and the present observations demonstrate the feasibility of this suggestion. Later, Mason et al. (1997) pointed out that bursts from Cyg X-1 could appear in the BATSE database; BATSE has indeed triggered

many times on this source. The long outbursts presented here have time histories which, if compressed in time, would be virtually impossible to distinguish from those of GRBs, and their spectra are hard. These similarities suggest that accretion onto a black hole, which is believed to power both Cyg X-1 and GRBs albeit under very different circumstances, may manifest itself in similar ways in very different settings.

5. Acknowledgments

Support for the *Ulysses* GRB experiment is provided by JPL Contract 958056, and for *Konus-Wind* by a Russian Aviation and Space Agency contract. We are grateful to Al Levine and the ASM/RXTE team for quick-look results on Cygnus X-1, and to Andrei Illarionov for useful discussions. This research has made use of the SIMBAD database, operated at CDS, Strasbourg, France.

REFERENCES

- Barrio F.E., Done, C., & Nayakshin, S., 2002, astro-ph/0209102
- Beloborodov, A.M., & Illarionov, A.F., 2001 MNRAS 323, 167
- Borkus, V. et al., 1995, Astron. Lett. 21, 794
- Cui, W., Feng, Y-X., and Ertmer, M., 2002, ApJ 564, L77
- Dove, J., Wilms, J., Nowak, M., Vaughan, B., and Begelman, M., 1998, MNRAS, 298, 729
- Frontera, F., et al., 2001, ApJ 546, 1027
- Giacconi, R., 1972, ApJ 173, 79
- Gierlinskii, M., et al., 1997, MNRAS 288, 958
- Gierlinskii, M., Zdziarskii, A., Poutanen, J., Coppi, S., Ebisawa, K., and Johnson, W.,
1999, MNRAS 309, 958
- Golenetskii, S., Aptekar, R., Mazets, E., Frederiks, Cline, T., and Hurley, K., 2002a,
IAU Circ. 7940
- Golenetskii, S., Aptekar, R., Mazets, E., Frederiks, Cline, T., and Hurley, K., 2002b, GCN
Circ. 1258 (<http://gcn.gsfc.nasa.gov/gcn3/1258.gcn3>)
- Hurley, K., Kouveliotou, C., Cline, T., Mazets, E., Golenetskii, S., Frederiks, D., and van
Paradijs, J., 1999, ApJ 523, L37
- Illarionov, A.,F., & Sunyaev, R.,A. 1975, A&A 39, 185
- Liang, E., and Nolan, P., 1984, Space Science Rev. 38, 353
- Ling, J., Mahoney, W., Wheaton, W., and Jacobson, A., 1987, ApJ 321, L117
- Ling, J. et al., 1997, ApJ 484, 375
- Maccarone, T., and Coppi, P., 2002, astro-ph/0204235

- Mazets, E., 1995, in AIP Conf. Proc. 384, Gamma-Ray Bursts - 3rd Huntsville Symposium,
Eds. C. Kouveliotou, M. Briggs, & G. J. Fishman (New York: AIP), 492
- Mason, P., McNamara, B., and Harrison, T., 1997, AJ 114(1), 238
- McConnell, M., et al., 2002, ApJ 572, 984
- Poutanen, J., Krolik, J., and Ryde, F., 1997, MNRAS 292, L21
- Romero, G., Kaufman Bernado, M., and Mirabel, I., 2002, astro-ph/0208495
- Schmidt, M., 2002, IAU Circ. 7856
- Stern, B., Beloborodov, A., and Poutanen, J., 2001, ApJ 555, 829
- Stirling, A., Spencer, R., de la Force, C., Garrett, M., Fender, R. and Ogley, R., 2001,
MNRAS 327, 1273
- Terekhov, M., Aptekar, R., Frederiks, D., Golenetskii, S., Il'inskii, V., and Mazets, E., 1998,
in AIP Conf. Proc. 428, Gamma-Ray Bursts - 4th Huntsville Symposium, Eds. C.
Meegan, R., Preece, & T. Koshut (New York: AIP), 894
- Zdziarski, A., Poutanen, J., Paciesas, W., and Wen, L., 2002, astro-ph/0204135
- Zhang, S., Cui, W., Harmon, A., Paciesas, W., Remillard, R., and van Paradijs, J., 1997,
ApJ 477, L95

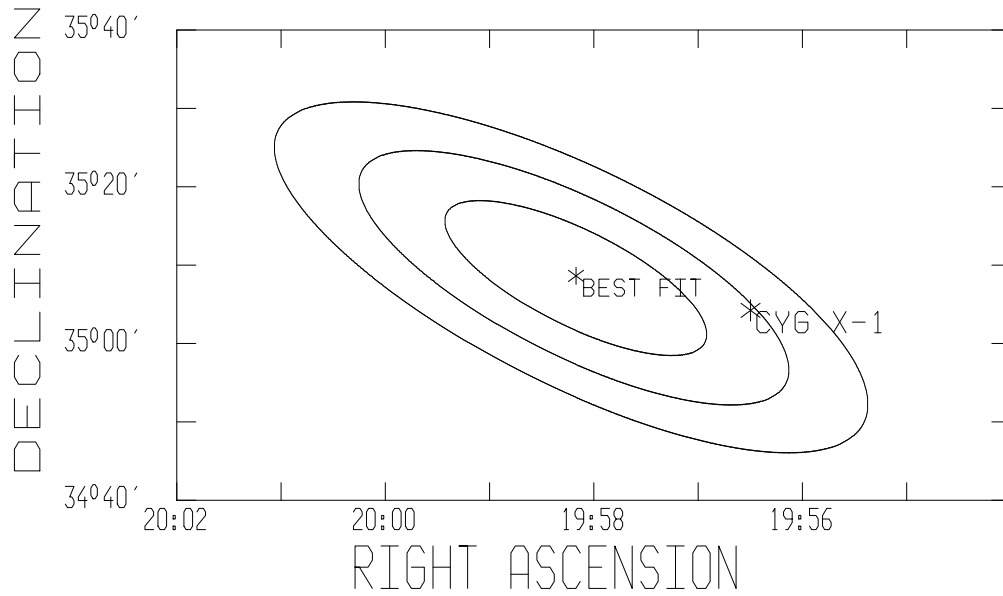


Fig. 1.— 1, 2, and 3 σ error ellipses for the six Cyg X-1 outbursts. Their areas are 328, 887, and 1700 square arcminutes. The best fit position is at $\alpha(2000) = 19^{\text{h}}58^{\text{m}}09^{\text{s}}$, $\delta(2000) = 35^{\circ}08'18''$, with a χ^2 of 4.01 for 4 degrees of freedom (6 annuli minus two fitting parameters). Cyg X-1 lies 0.35° away, at the $\sim 95\%$ confidence level. A search through the SIMBAD database has not identified any other X-ray sources within the 3σ error ellipse.

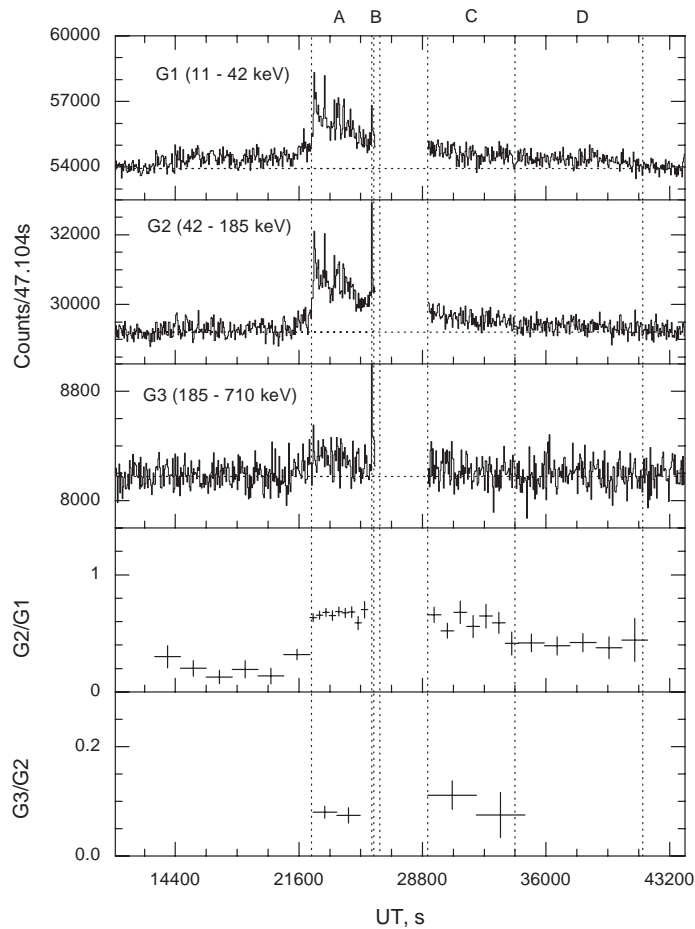


Fig. 2.— The Cyg X-1 outburst on 950325 as observed by *Konus-Wind*. The time histories are shown in the three energy bands G1, G2, and G3 with time resolution 47.104 s; the hardness ratios $G2/G1$ and $G3/G2$ are also shown. A, B, C, and D denote the time intervals where the spectral parameters were estimated. The narrow spike at 25841 s in the beginning of interval B is the GRB which triggered a series of multichannel spectra measurements, covering the entire interval B. The gap after B was caused by the transmission of high resolution data to the onboard tape recorder. Background levels are indicated by the dashed lines.

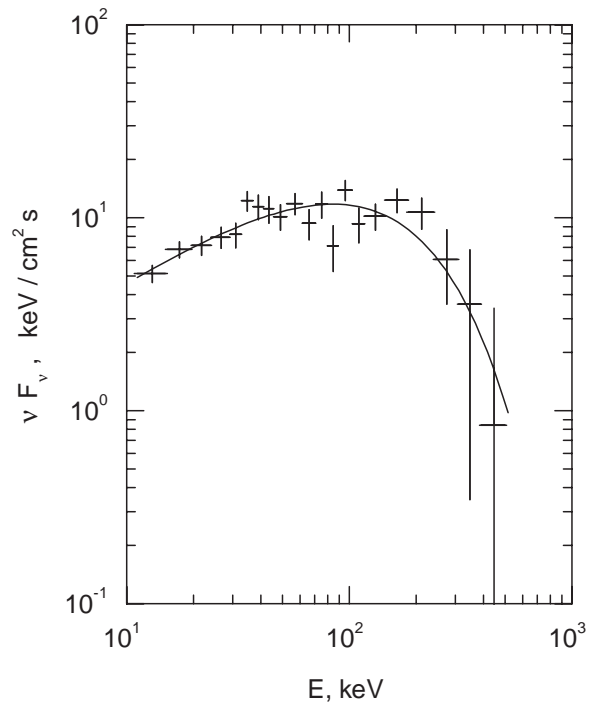


Fig. 3.— KONUS νF_ν spectrum of the outburst on 950325. The spectrum was accumulated at the decay stage of the flare during 360 s of interval B with moderate statistics. The solid curve is the result of the spectral fit; $\chi^2 = 22.6$ for 18 degrees of freedom. The spectral shape is consistent with that of the hard state of Cyg X-1.

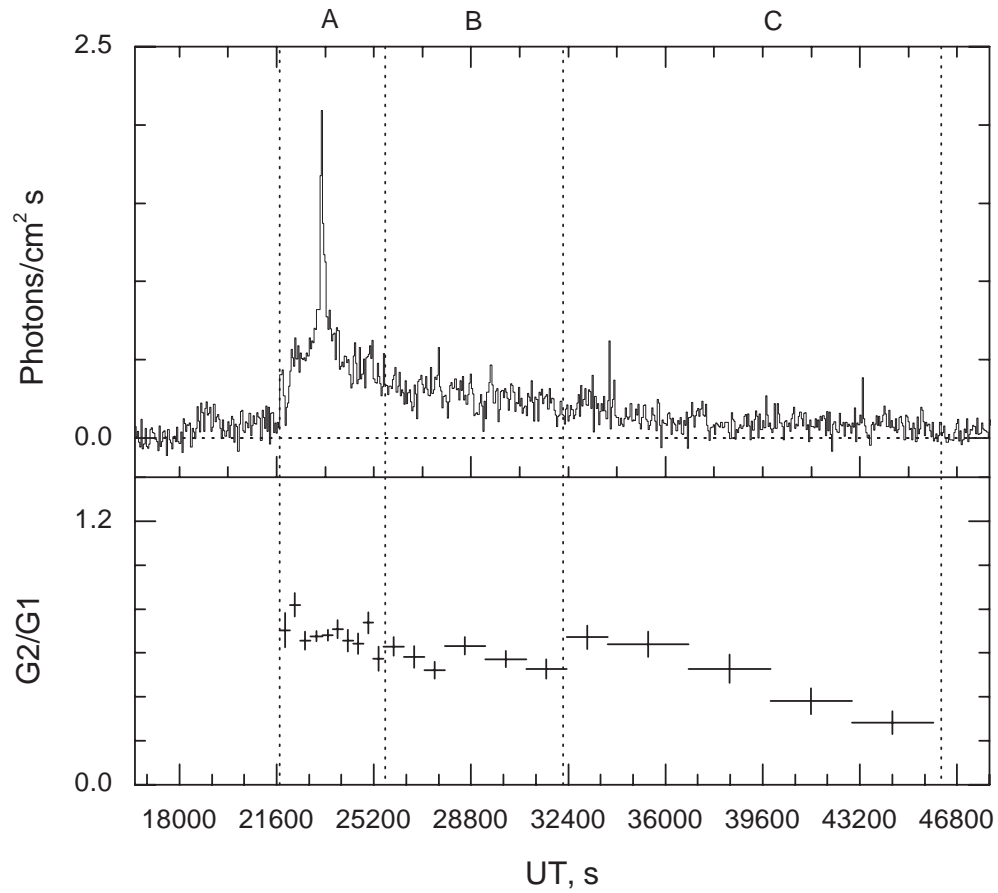


Fig. 4.— Konus 15 - 300 keV time history, and the hardness ratio, of the flare on 950110. Spectral fits were done for intervals A, B, C, and A+B+C. The photon fluxes in photons $\text{cm}^{-2} \text{s}^{-1}$ were calculated by deconvolving the count rate data. The time resolution is 47.104 s. The background level is indicated by the dashed line.

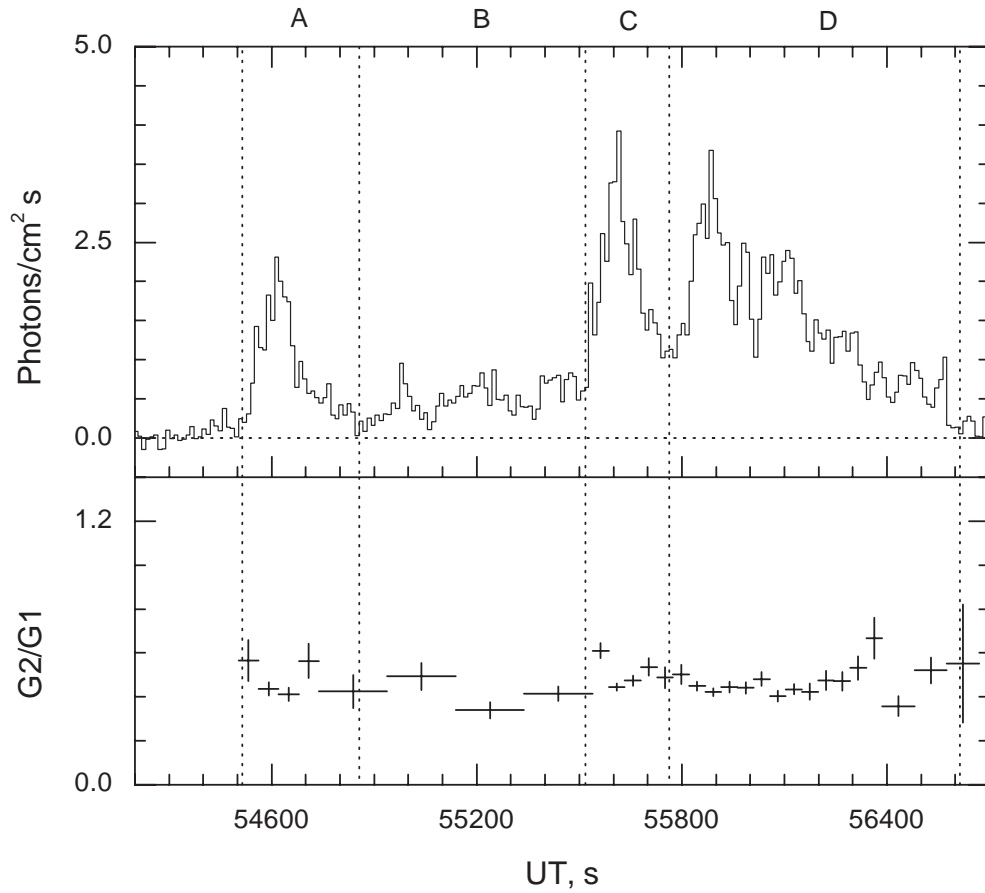


Fig. 5.— Konus 15 - 300 keV photon fluxes and hardness ratios for the outburst on 990421A. The time resolution is 11.776 s. Spectral fits were done for intervals A, B, C, D, and A+B+C+D. The background level is indicated by the dashed line.

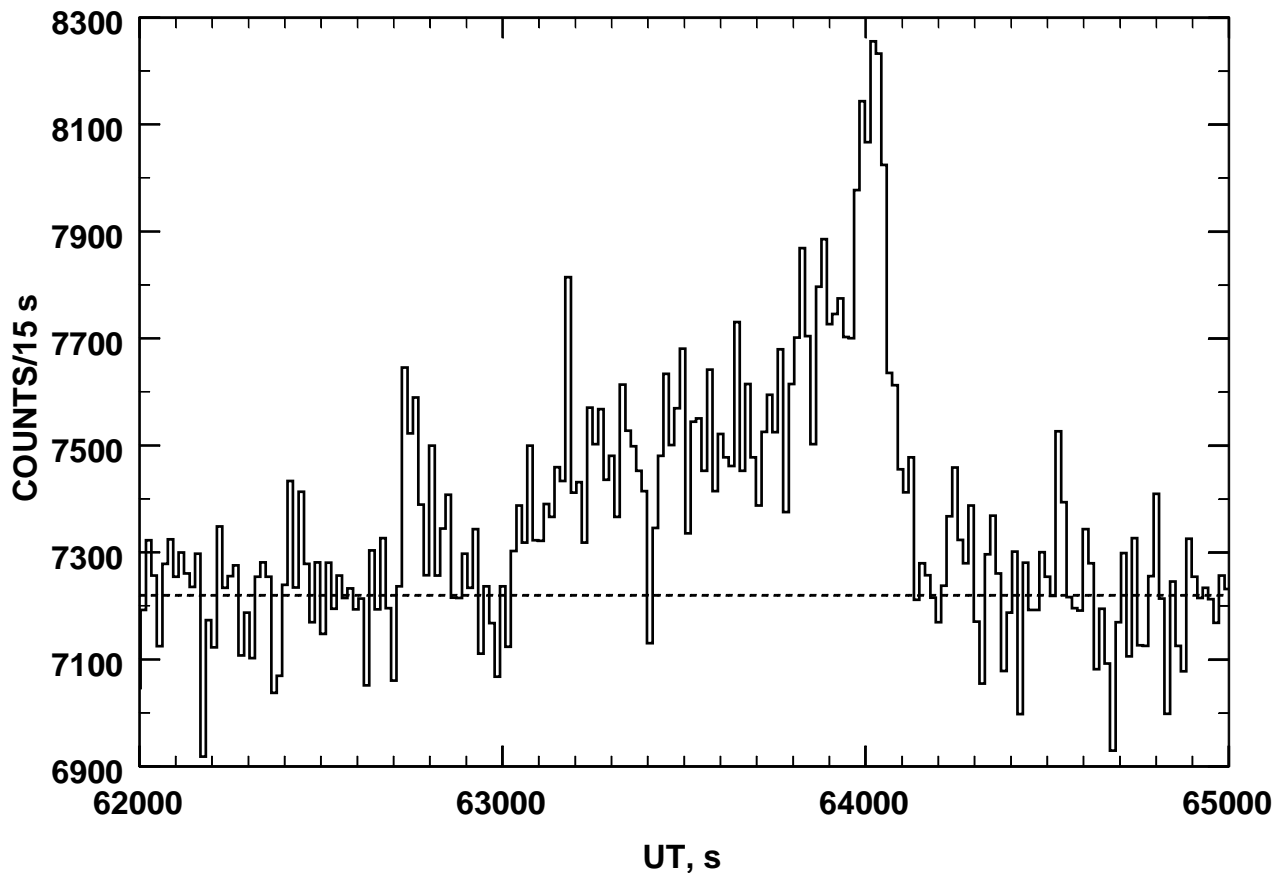


Fig. 6.— *Ulysses* 25 - 150 keV count rates for the outburst on 990421B. The time resolution is 15 s. Note that the onset is several hundred seconds prior to the onset at BATSE (Stern et al. 2001), due to Earth occultation. No *Ulysses* spectral data is available for this outburst. Due to the proximity in time to the previous outburst, the two could be considered manifestations of a single episode, although the Konus and *Ulysses* count rates remained at their background levels between them. In contrast to the outbursts on 950110, 950325, 990421A, and 020224, this time history exhibits a slow rise and a fast decay. The background level is indicated by the dashed line.

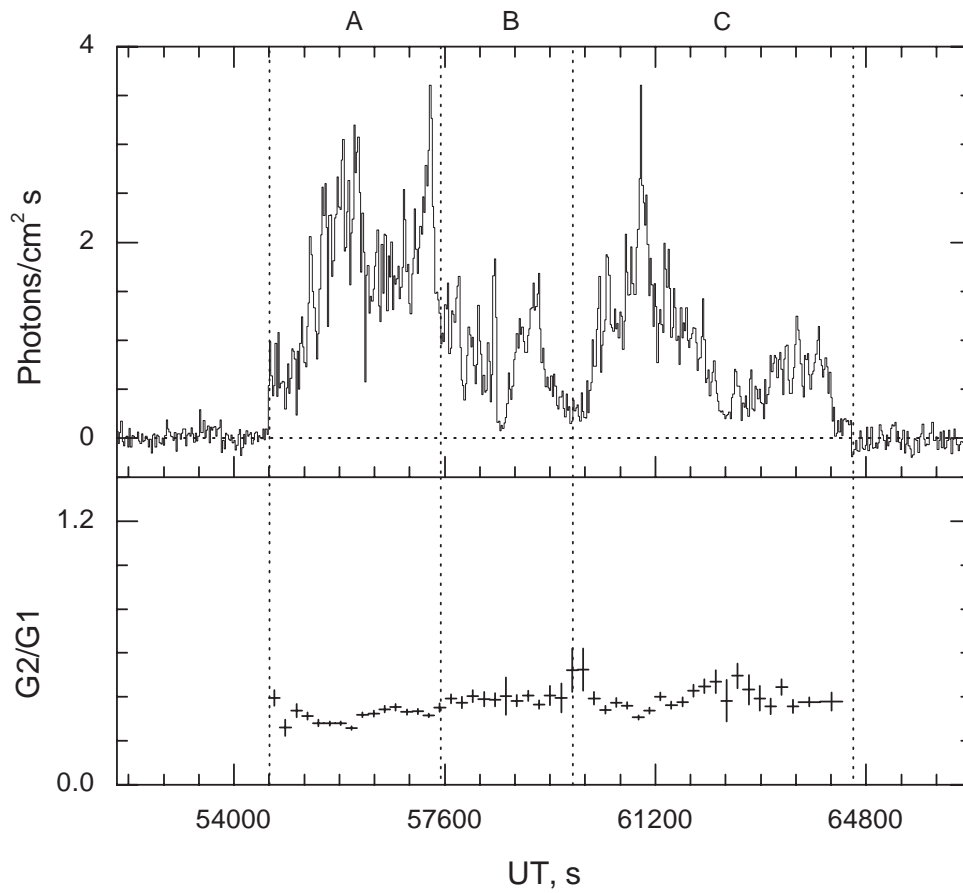


Fig. 7.— Konus 15-300 keV photon fluxes and hardness ratios for the outburst on 020224. The time resolution is 23.552 s. Spectral fits were done for intervals A, B, C, and A+B+C. The background level is indicated by the dashed line.

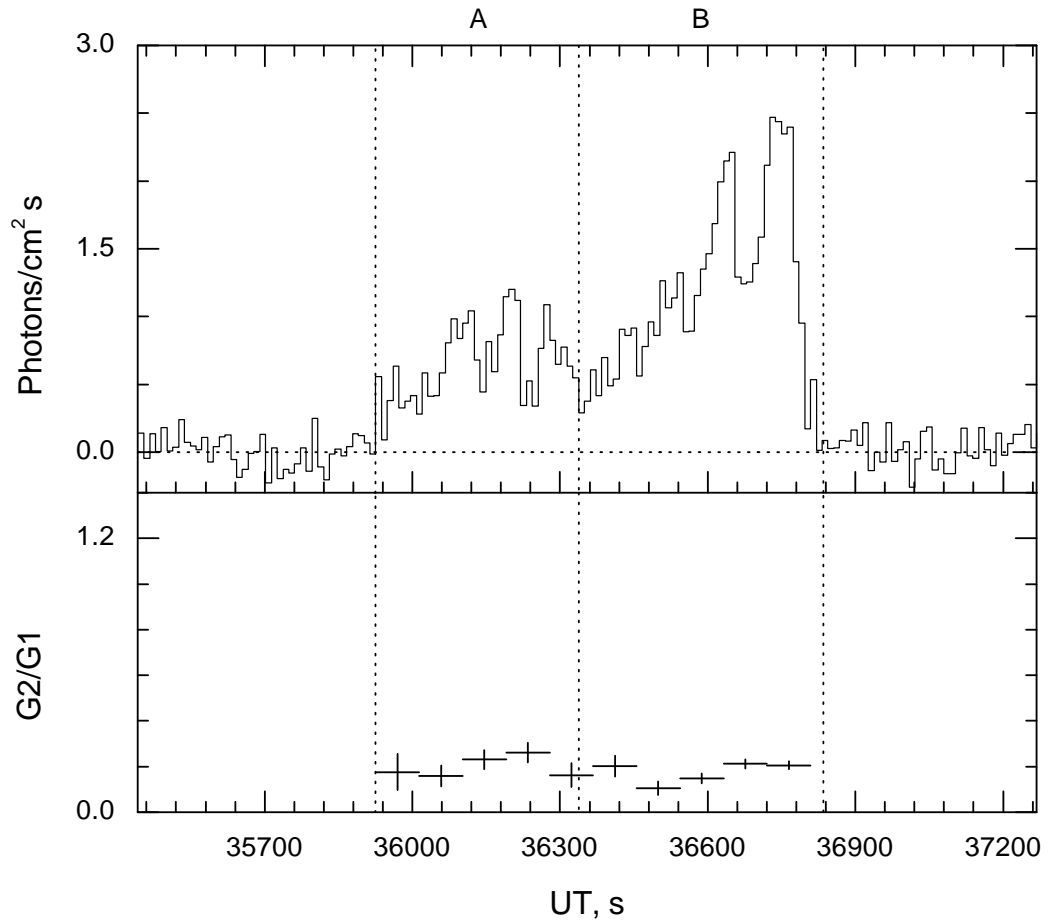


Fig. 8.— Konus 15-300 keV photon fluxes and hardness ratios for the outburst on 020331. The time resolution is 11.776 s. Spectral fits were done for intervals A, B, and A+B. The background level is indicated by the dashed line. Note the resemblance to the time history of 990421B (slow rise, fast decay).

Table 1. *Six Cygnus X-1 outbursts*

Date (YYMMDD)	UT, start	Duration, s (approximate)	Spacecraft	Underlying spectral state
950110	18600	27500	<i>Ulysses</i> ^a , Konus ^{a,b} , BATSE ^c	hard
950325	14400	28000	<i>Ulysses</i> ^a , Konus ^{a,b} , BATSE ^c	hard
990421A	54510	4870	<i>Ulysses</i> , Konus, BATSE ^d	hard
990421B ^e	63100	1360	<i>Ulysses</i> , BATSE ^d	hard
020224	54600	10000	<i>Ulysses</i> ^a , Konus ^b	soft
020331	35925	910	<i>Ulysses</i> , Konus	soft

^aGolenetskii et al. (2002a,b)

^bMazets et al. (1995)

^cSchmidt (2002)

^dStern, Beloborodov, and Poutanen (2001)

^eThis event may be a continuation of the preceding one.

Table 2. *Energy spectra from Konus - Wind*

Date	Time interval (see figures 2-7)	A, photons cm ⁻² s ⁻¹	α	E ₀ , keV	E _p , keV
950110	A	0.92±0.12	1.25±0.04	115±9	86±8
	B	0.89±0.19	1.45±0.07	135±22	74±15
	C	0.99±0.30	1.80±0.07	450±21	90±32
	A+B+C	0.83±0.08	1.50±0.04	160±16	80±10
950325	A	0.92±0.13	1.25±0.05	110±10	82±9
	B ^a	0.88±0.15	1.24±0.15	112±29	85±27
	B ^b	0.77±0.20	1.28±0.18	156±60	112±52
	C	0.64±0.18	1.50±0.11	155±43	78±27
	D	0.94±0.40	1.80±0.25	165±130	33±49
	A+C+D	0.59±0.11	1.40±0.05	130±16	78±27
990421A	A	1.40±0.85	1.20±0.39	85±48	68±51
	B	4.20±1.7	1.80±0.12	435±275	87±76
	C	10.70±1.6	1.65±0.05	300±54	105±24
	D	2.80±0.9	1.30±0.11	110±20	77±19
	A+B+C+D	3.90±0.6	1.50±0.05	165±20	83±13
020224	A	2.30±1.5	1.10±0.35	64±20	58±29
	B	0.50±0.4	0.90±0.49	64±30	70±46
	C	2.90±0.9	1.45±0.21	120±25	66±29

Table 2—Continued

Date	Time interval (see figures 2-7)	A, photons cm ⁻² s ⁻¹	α	E ₀ , keV	E _p , keV
	A+B+C	2.40±0.9	1.30±0.15	90±13	63±16
020331	A	57.00±12	2.50±0.08		
	B	145.00±19	2.60±0.05		
	A+B	97.00±13	2.55±0.04		

^aMultichannel spectrum

^b3 channel spectrum

Table 3. *Fluences and peak fluxes from Konus - Wind*

Date	Time interval, s	15 - 300 keV		Luminosity at 2 kpc erg s ⁻¹
		fluence erg cm ⁻²	peak flux photons cm ⁻² s ⁻¹ erg cm ⁻² s ⁻¹	
950110	21712 - 46215	4.5×10^{-4}	2.4 1.9×10^{-7}	9.1×10^{37}
950325	22331 - 42635	2.8×10^{-4}	1.3 9.5×10^{-8}	4.6×10^{37}
990421A	54514 - 56613	1.8×10^{-4}	3.8 3.0×10^{-7}	1.4×10^{38}
020224	54609 - 64583	8.0×10^{-4}	3.7 2.7×10^{-7}	1.3×10^{38}
020331	35926 - 36835	4.7×10^{-5}	2.4 1.3×10^{-7}	6.2×10^{37}